Rev. Roum. Sci. Techn.– Électrotechn. et Énerg.
Vol. 71, 3, pp. 415–420, Bucarest, 2026

JOINT FRACTIONAL-ORDER MODELING AND KALMAN FILTERING FOR BATTERY STATE-OF-CHARGE ESTIMATION

FETHI LAKHDARI[1]

Keywords: Lithium-ion battery; Fractional-order model; Extended Kalman filter; Parameter identification; Grünwald–Letnikov derivative.

Accurate state-of-charge (SOC) estimation is critical for reliable battery management. To address the limitations of conventional models, this paper presents a robust adaptive estimation framework that combines fractional-order modeling with extended Kalman filtering (EKF). The approach uses a computationally efficient fractional-order equivalent circuit model (FO-ECM) to represent nonlinear battery behavior. Its key innovation is augmenting the EKF's state vector to jointly estimate SOC and slowly varying internal resistances, enabling real-time model adaptation to aging and temperature changes without separate health monitoring. Validated under dynamic loads and varying temperatures, the framework achieves SOC estimation with root mean square error (RMSE) consistently below 3.5% and robust convergence despite noise and initial uncertainty.

1. INTRODUCTION

Lithium-ion batteries (LIBs) power applications from portable electronics to electric vehicles, with performance critically dependent on accurate state-of-charge (SOC) estimation by the battery management system (BMS) [1,2].

However, sustained SOC accuracy remains challenging due to LIBs complex nonlinear behavior—diffusion, memory effects, and parameter variations from aging and temperature [3,4].

Fixed offline models inevitably degrade over time. While physics-based electrochemical models offer high fidelity, their computational demands preclude real-time implementation. Conversely, conventional integer-order equivalent circuit models (ECMs) are efficient but oversimplify battery dynamics [5]; improving accuracy requires added complexity. Fractional-order models (FOMs) provide an elegant compromise, using non-integer calculus to describe distributed relaxation and diffusion with parsimonious structure [6,7]. A prevalent implementation uses Constant Phase Elements (CPEs), whose impedance is:

$$Z_{CPE}=\frac{1}{Q(\mathrm{j}\omega)^{\alpha}}\ ,\ 0<\alpha<1. \tag{1}$$

where Q is pseudo-capacitance and α is the fractional order. The superiority of CPE-based FOMs is well-documented: [8] showed fractional-order models outperforming integer-order ECMs under dynamic profiles, while [9,10] confirmed that Fractional-Order Equivalent Circuit Models (FO-ECMs) capture distributed time constants more efficiently. Meta-heuristic techniques achieve 98% fit to electrochemical impedance spectroscopy data [11]. Fractional-order methods have also proven effective in control applications, including EV charging systems [12] and predictive control of nonlinear fractional models [13–15].

Despite advances in modeling, a gap remains: most studies treat FO-ECM parameters as static, yet sustained accuracy requires adaptation to parameter drift. While extended Kalman filtering (EKF) is foundational for SOC estimation [16], its fractional-order application lacks a unified joint state-parameter strategy. This paper addresses this gap with a framework that combines FO-ECM and a joint state-parameter EKF.

The paper's main contributions are: (i) joint EKF with augmented state (SOC and slowly varying parameters); (ii) systematic FO-ECM identification from discharge/rest data; (iii) experimental validation with sustained SOC accuracy (RMSE < 3.5%).

The paper is organized as follows: Section 2 presents fractional calculus. Sections 3-4 detail the FO-ECM and parameter identification. Section 5 describes the joint EKF framework. Section 6 presents experimental validation. Section 7 concludes.

2. THEORETICAL BACKGROUND: FRACTIONAL CALCULUS

Fractional calculus generalizes differentiation and integration to non-integer orders, providing a framework for modeling systems with hereditary and memory effects [17].

The fractional derivative of a function $f(t)$ of order α is denoted as:

$$D^{\alpha}=\frac{\mathrm{d}^{\alpha}f(t)}{\mathrm{d}t^{\alpha}},\alpha\in\mathbb{R}^{+}. \tag{2}$$

Several definitions exist, with the most common being the Riemann-Liouville, Caputo, and Grünwald-Letnikov (GL) definitions. This work employs the GL definition due to its inherent suitability for direct digital implementation and straightforward discrete-time representation, which is essential for real-time BMS algorithms.

2.1 GRÜNWALD–LETNIKOV DEFINITION

For a real order α, the GL fractional derivative is defined as:

$$D^{\alpha}x(t)\approx\lim_{h\to 0}\frac{1}{h^{\alpha}}\sum_{j=0}^{k}(-1)^{j}\binom{\alpha}{j}f(t-jh)\,. \tag{3}$$

where h is the step size and the binomial coefficient (4) for a real order α is calculated using the Gamma function Γ(x) defined in (5).

$$\binom{\alpha}{j}=\frac{\Gamma(\alpha+1)}{\Gamma(j+1)\Gamma(\alpha-j+1)}. \tag{4}$$

$$\Gamma(x)=\int_{0}^{\infty}t^{x-1}\,\mathrm{e}^{-t}\mathrm{d}t,x\in\mathbb{R}. \tag{5}$$

For practical digital implementation, the derivative at the k-th time step is approximated by truncating the infinite series to a finite memory length L:

$$D^{\alpha}x_{k}\approx\frac{1}{h^{\alpha}}\sum_{j=0}^{L}(-1)^{j}\binom{\alpha}{j}x_{k-j}=\frac{1}{h^{\alpha}}\sum_{j=0}^{L}\omega_{j}(\alpha)\,x_{k-j}. \tag{6}$$

where $\omega_j(\alpha)$ are the GL coefficients. This recursive kernel

[1] LEPESA laboratory, University of Sciences and Technology (USTO), Oran, Algeria, fethi.lakhdari@univ-usto.dz

DOI: 10.59277/RRST-EE.2026.3.13

embeds the system's memory, as the current state depends on a weighted sum of L past states. The selection of L represents a critical trade-off between model accuracy and computational burden.

2.2 FRACTIONAL-ORDER STATE-SPACE MODEL

To integrate fractional-order dynamics with state estimation algorithms, a discrete-time fractional-order state-space model is derived. The general linear discrete state-space model is written as:

$$\begin{cases} D^{\alpha}\,\mathbf{x}_{k+1} = \mathbf{A}\,\mathbf{x}_k + \mathbf{B}\,\mathbf{u}_k. \\ \mathbf{y}_k = \mathbf{C}\,\mathbf{x}_k\,, \end{cases} \tag{7}$$

where the state vector is $\mathbf{x}_k$, $\mathbf{u}_k$ the input, and $\mathbf{y}_k$ the output. $\boldsymbol{\alpha} = [\alpha_1, \dots, \alpha_N]^{\mathrm{T}}$ are the fractional-order derivatives.

By applying the GL definition from (6) to the state equation in (7), we obtain:

$$\mathbf{H}\sum_{j=0}^{L} \boldsymbol{\Omega}_j(\alpha)\,\mathbf{x}_{k+1-j} = \mathbf{A}\,\mathbf{x}_k + \mathbf{B}\,\mathbf{u}_k\,. \tag{8}$$

where $\boldsymbol{\Omega}_j(\alpha)$ is the diagonal Newton binomial matrix $\left(\mathrm{diag}\left[\binom{\alpha_1}{j} \dots \binom{\alpha_N}{j}\right]\right)$, and $\mathbf{H}$=diag$\left[1/h^{\alpha_1} \dots 1/h^{\alpha_N}\right]$.

Noting that $\boldsymbol{\Omega}_0(\alpha)$ =$\mathbf{I}$ (identity matrix), and isolating the current state $\boldsymbol{x}_{k+1}$ yields the recursive form:

$$\mathbf{x}_{k+1} = \mathbf{H}\,\mathbf{A}\,\mathbf{x}_k - \sum_{j=1}^{L} \boldsymbol{\Omega}_j(\alpha)\,\mathbf{x}_{k+1-j} + \mathbf{H}\,\mathbf{B}\,\mathbf{u}_k. \tag{9}$$

Define $\boldsymbol{A}_f = \mathbf{H}\,\boldsymbol{A}$, and $\boldsymbol{B}_f = \mathbf{H}\,\boldsymbol{B}$. Incorporating process noise $\mathbf{w}_k$ and measurement noise $\mathbf{v}_k$ (zero-mean Gaussian with covariances $\mathbf{Q}_k$ and $\mathbf{R}_k$), the stochastic fractional-order state-space model is:

$$\begin{cases} \mathbf{x}_{k+1} = \mathbf{A}_f\mathbf{x}_k - \displaystyle\sum_{j=1}^{L} \boldsymbol{\Omega}_j(\alpha)\;\mathbf{x}_{k+1-j} + \mathbf{B}_f\mathbf{u}_k + \mathbf{w}_k, \\ \mathbf{y}_k = \mathbf{C}\,\mathbf{x}_k + \mathbf{v}_k. \end{cases} \tag{10}$$

The summation term $-\sum_{j=1}^{L}\boldsymbol{\Omega}_j(\alpha)\;\mathbf{x}_{k+1-j}$ is the hallmark of the fractional model, encapsulating the system's infinite memory by coupling the current state to a long history of its past values. This property is essential for accurately modeling the dynamical behavior of lithium-ion battery reactions.

3. PROPOSED FRACTIONAL-ORDER BATTERY MODELING

In the current study, the lithium-ion cell is described using a fractional-order equivalent circuit model (FO-ECM) that captures both instantaneous and long-memory dynamics. The model, illustrated in Fig. 1, comprises:

- Open-circuit voltage source (*OCV(SOC)*): modeling the thermodynamic equilibrium potential as a function of SOC.
- Ohmic resistor (R_0): A series resistor modeling the immediate voltage drop due to electronic and ionic conduction paths.
- Leakage resistor (R_{leak}): A parallel resistor modeling the battery power leakage process.
- Parallel Branch (R_1-*CPE*): A parallel combination of a resistor and constant phase element modeling distributed polarization dynamics.

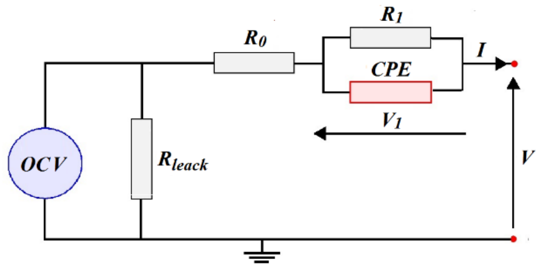

Fig. 1 – The proposed fractional-order circuit model (FO-ECM) for a lithium-ion battery.

The proposed fractional-order equivalent circuit model is governed by the following continuous-time equations:

- SOC dynamics:

$$\frac{\mathrm{d}\,SoC}{\mathrm{d}t} = -\frac{1}{C_n}\left(I(t) + \frac{OCV(SOC)}{R_{leak}}\right). \tag{11}$$

where C_n is the nominal capacity (in Ah), $I(t)$ applied current (positive for discharge).

- Fractional-state dynamics:

$$D^{\alpha}V_1(t) = -\frac{1}{R_1Q_1}V_1(t) + \frac{1}{Q_1}I(t), \tag{12}$$

where, $V_1(t)$ is the voltage across R_1-*CPE* branch, R_1 the polarization resistance, and Q_1 the pseudo-capacitance.

- Output voltage equation:

$$V(t) = OCV(SOC) - R_0I(t) - V_1(t). \tag{13}$$

Applying the GL definition (6) to the fractional-state dynamics in (12) yields the discrete-time equivalent for V_1:

$$V_1[k] = \frac{1}{h^{\alpha}}\sum_{j=0}^{L}\omega_j(\alpha)\;V_1[k\text{-}j] = -\frac{1}{R_1Q_1}V_1[k] + \frac{1}{Q_1}I[k]\,. \tag{14}$$

After rearrangement:

$$V_1[k] = -\sum_{j=1}^{L}\Phi(j)\,V_1[k-j] + \frac{1}{A_1}I[k], \tag{15}$$

where:

$$\Phi(j) = \frac{S_1\omega_j(\alpha)}{A_1},\; S_1 = \frac{Q_1}{h^{\alpha}},\; A_1 = S_1 + \frac{1}{R_1}, \tag{16}$$

and $\omega_j(\alpha)$ is approximated by:

$$\omega_j(\alpha) = (-1)^j\binom{\alpha}{j} = (-1)^j\,\frac{\alpha(\alpha-1)\dots(\alpha-j+1)}{j!}. \tag{17}$$

A state vector is defined as:

$$\mathbf{x}_v[k] = [\mathrm{V}_1(k), \mathrm{V}_1(k-1), \dots, \mathrm{V}_1(k-L+1)]^{\mathrm{T}}. \tag{18}$$

This leads to a standard state-space representation:

$$\begin{cases} \mathbf{x}_v[k+1] = \mathbf{A}_v\mathbf{x}_v[k] + \mathbf{B}_v\,\mathrm{I}[k], \\ \mathrm{z}_v[k] = \mathbf{C}_v\mathbf{x}_v[k], \end{cases} \tag{19}$$

where the system matrices are explicitly defined as:

$$\begin{cases} \mathbf{A}_v = \begin{bmatrix} -\Phi(1) & -\Phi(2) & \ldots & -\Phi(L\text{-}1) & -\Phi(L) \\ 1 & 0 & \ldots & 0 & 0 \\ 0 & 1 & \ldots & 0 & 0 \\ \vdots & \vdots & \vdots & \vdots & \vdots \\ 0 & 0 & 0 & 1 & 0 \end{bmatrix}. \\ \mathbf{B}_v = \left[\frac{1}{A_1}, 0, \ldots, 0\right]^{\mathrm{T}} \\ \mathbf{C}_v = [1, 0, \ldots, 0] \end{cases} \tag{20}$$

where the output variable z_v is the fractional element voltage (*i.e.*, V_1).

4. MODEL PARAMETER IDENTIFICATION

A sequential identification procedure exploits the discharge/rest protocol to decouple static, linear, and fractional dynamics, identifying parameters in order of decreasing time constants: instantaneous effects, slow leakage, and fractional polarization dynamics. The static parameters are identified as follows:

- The *OCV*(*SOC*) is obtained by fitting a piecewise linear function to voltage-SOC data from low-current rest periods during discharge.
- The ohmic resistance: R_0 is estimated as the median of $|\Delta V/\Delta I|$ across significant current steps, using averaged values to reduce noise.
- The leakage resistance: R_{leak} is identified by analyzing slow self-discharge during extended rest periods where external current is approximately zero. Under this condition, equation (11) simplifies to:

$$\frac{\mathrm{d}\,SOC}{\mathrm{d}t} = -\frac{OCV}{C_n\, R_{leak}}. \tag{21}$$

Linear regression applied to data from multiple rest periods yields a reliable R_{leak} value.

The identification of fractional-order parameters (R_1,Q_1,α) is intrinsically linked to selecting the memory length L in the discrete-time Grünwald-Letnikov implementation. This selection fundamentally balances model accuracy against computational complexity.

To isolate the polarization voltage, z_v, the self-discharge effect is compensated by correcting the state of charge value SOC_{corr} using the identified R_{leak}. The detrended relaxation signal is then:

$$z_v[k] = OCV(SOC_{corr}[k]) - V_{meas}[k], \tag{22}$$

where V_{meas} is the measured terminal voltage. $z_v[k]$ is then modeled as an autoregressive AR process of order L:

$$z_v[k] = \sum_{j=1}^{L} \Phi(j) z_v[k-j] + \varepsilon[k], \tag{23}$$

where Φ are the AR coefficients, and ε is the white noise residual.

The optimal memory length is determined as follows: for candidate lengths $L = 1 \ldots M_{max}$, $AR(m)$ models are fitted. The optimal order M_{opt} is selected by minimizing both the Akaike information criterion (AIC) (24), and the Bayesian Information Criterion (BIC) (25) [18,19]:

$$AIC(m) = N \ln(\sigma_m^2) + 2\,m, \tag{24}$$

$$BIC(m) = N \ln(\sigma_m^2) + m \ln(N), \tag{25}$$

where N is the data points, and σ_m^2 is the residual variance. The candidate optimal orders are:

$$\begin{cases} M_{opt}^{AIC} = \arg\min_{\mathrm{m}} AIC(m), \\ M_{opt}^{BIC} = \arg\min_{\mathrm{m}} BIC(\mathrm{m}). \end{cases} \tag{26}$$

To ensure significant improvement, the selected M_{opt} must satisfy:

$$\frac{\mathrm{RMSE}(M_{opt}^{AIC})}{\mathrm{RMSE}(M_{opt}^{AIC} - 1)} \le \eta, \tag{27}$$

where η = 0.95 requires at least 5% improvement.

Once M_{opt} is determined, the core identification step maps the statistically estimated AR coefficients Φ to the theoretical dynamics of the FO-ECM. From the analytical solution (14), the theoretical AR coefficients for polarization voltage are:

$$\Phi(\mathrm{j}) = -\frac{S_1 \omega_j(\alpha)}{A_1}. \tag{28}$$

The parameters (R_1,Q_1,α) are identified by solving:

$$\min f(R_1, Q_1, \alpha) = \sum_{j=1}^{M_{\mathrm{opt}}} \left(\Phi_j^{AR} + \frac{S_1}{A_1}\omega_j(\alpha)\right)^2. \tag{29}$$

This minimization is performed via constrained search: a coarse grid search over α ∈ (0, 1) followed by local refinement (*e.g.*, gradient-based method) to obtain precise optimal parameters.

5. JOINT STATE-PARAMETER EKF FRAMEWORK

The EKF is employed for simultaneous, real-time estimation of SOC and slowly varying battery parameters [20]. By linearizing nonlinear dynamics around the current state estimate at each step [21], the EKF provides a computationally efficient solution for BMS. Similar joint estimation approaches have been explored in aerospace applications [22] and fractional-order control systems [23].

Consider the discrete-time nonlinear system:

$$\begin{cases} \mathbf{x}_k = f(\mathbf{x}_{k-1}, \mathbf{u}_{k-1}) + \mathbf{w}_{k-1}, \\ \mathbf{y}_k = h(\mathbf{x}_k, \mathbf{u}_{k)}) + \mathbf{v}_k, \end{cases} \tag{30}$$

where $\boldsymbol{x}_k$ is state, $\mathbf{u}_k$ input, $\mathbf{y}_k$ output, and *f*, *h* nonlinear functions. $\mathbf{w}_k$ and $\mathbf{v}_k$ are zero-mean Gaussian with covariances $\mathbf{Q}_k$ and $\mathbf{R}_k$.

The EKF algorithm proceeds recursively in a predict-update cycle as follows:

Prediction step:

$$\begin{cases} \hat{\mathbf{x}}_{k|k-1} = f(\hat{\mathbf{x}}_{k-1|k-1}, \mathbf{u}_{k)}), \\ \mathbf{P}_{k|k-1} = \mathbf{F}_k \mathbf{P}_{k-1|k-1} \mathbf{F}_k^T + \mathbf{Q}_k. \end{cases} \tag{31}$$

Update step:

$$\begin{cases} \tilde{\mathbf{y}}_k = \mathbf{y}_k - h(\hat{\mathbf{x}}_{k|k-1}, \mathbf{u}_k), \\ \mathbf{S}_k = \mathbf{H}_k \mathbf{P}_{k|k-1} \mathbf{H}_k^T + \mathbf{R}_{k.} \end{cases} \tag{32}$$

Compute the optimal Kalman gain:

$$\mathbf{K}_k = \mathbf{P}_{k|k-1} \mathbf{H}_k^T {\mathbf{S}_k}^{-1}. \tag{33}$$

Update the a posteriori state and covariance estimates:

$$\begin{cases} \hat{\mathbf{x}}_{k|k} = \hat{\mathbf{x}}_{k|k-1} + \mathbf{K}_k \hat{\mathbf{y}}_k, \\ \mathbf{P}_{k|k} = (\mathbf{I} - \mathbf{K}_k \mathbf{H}_k)\mathbf{P}_{k|k-1}. \end{cases} \tag{34}$$

$\mathbf{F}_\mathrm{k}$ and $\mathbf{H}_\mathrm{k}$ are the Jacobians of the nonlinear functions f and h, respectively, linearized around the current state estimate:

$$\mathbf{F}_k = \left.\frac{\partial f}{\partial \mathbf{x}}\right|_{\hat{\mathbf{x}}_{k|k-1}, \mathbf{u}_k}, \ \mathbf{H}_k = \left.\frac{\partial h}{\partial \mathbf{x}}\right|_{\hat{\mathbf{x}}_{k|k-1}, \mathbf{u}_k}. \tag{35}$$

An augmented state vector is constructed, enabling joint estimation of the battery SOC, and some model parameters:

$$\mathbf{x} = [SOC, \mathbf{x}_v^\mathrm{T}, R_0, R_{leak}]^\mathrm{T}. \tag{36}$$

where $\mathbf{x}_v$ is the state vector for the fractional branch defined in eq. (18).

The state transition equations are:

$$\begin{cases} SOC[k+1] = SOC[k] - \dfrac{h}{C_n} I[k] - \dfrac{OCV(SOC[k])}{R_{leak}[k]} \\ \qquad + w_1 \\ \mathbf{x}_v[k+1] = \mathbf{A}_v \mathbf{x}_v[k] + \mathbf{B}_v I[k] + w_2, \\ R_0[k+1] = R_\mathbf{0}[k] + w_3, \\ R_{leak}[k+1] = R_{leak}[k] + w_4. \end{cases} \tag{37}$$

The measurement equation is:

$$\mathbf{y}[k] = OCV(SOC[k]) - R_0[k]\, I[k] - \mathbf{C}_v \mathbf{x}_v[k], \tag{38}$$

where $\mathbf{A}_v$, $\mathbf{B}_v$ and $\mathbf{C}_v$ are matrices defined in (20).

Finally, the Jacobians $\mathbf{F}_k$ and $\mathbf{H}_k$ are computed by differentiating eq. (37), and (38) with respect to the state vector:

$$\mathbf{F}_k = \begin{bmatrix} (1 - \dfrac{h}{C_\mathrm{n} R_{leak}}) \dfrac{\partial OCV}{\partial SOC} & \mathbf{0}_{1\mathrm{x}L} & 0 & \dfrac{h}{C_\mathrm{n}} \dfrac{OCV}{R_{leak}^2} \\ \mathbf{0}_{L\mathrm{x}1} & \mathbf{A}_v & \mathbf{0}_{L\mathrm{x}1} & \mathbf{0}_{L\mathrm{x}1} \\ 0 & \mathbf{0}_{1\mathrm{x}L} & 1 & 0 \\ 0 & \mathbf{0}_{1\mathrm{x}L} & 0 & 1 \end{bmatrix}, \tag{39}$$

$$\boldsymbol{H}_k = \begin{bmatrix} \dfrac{\partial OCV}{\partial SOC} & -\mathbf{C}_v & -\mathbf{I}[k] & 0 \end{bmatrix}. \tag{40}$$

6. EXPERIMENTAL VALIDATION AND DISCUSSION

The proposed framework was evaluated through controlled laboratory testing and standardized benchmark data to assess model fidelity, parameter identification accuracy, and SOC estimation performance under diverse conditions. Temperature effects on battery performance were considered, as highlighted in recent studies [4].

A test bench was developed with commercial 18650 lithium-ion battery packs (2.5 Ah, 14.8V), a programmable electronic load, and data acquisition. Voltage and current were recorded at 1 Hz. The procedure began with a fully charged battery, followed by an open-circuit rest to reach electrochemical equilibrium. Sequential characterization cycles with constant-current discharge pulses and rest periods (Fig. 2) yielded voltage-relaxation characteristics for parameter estimation across SOC levels.

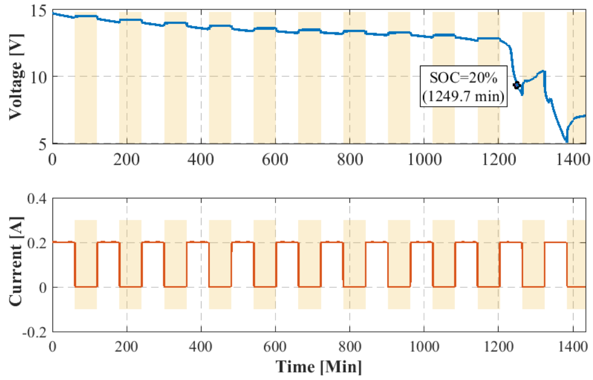

Fig. 2 – Cyclic discharge/rest test: voltage (top) and current (bottom).

The OCV-SOC relationship (Fig. 3) shows a linear behavior over a wide range with a slope change in the vicinity of 20% SOC.

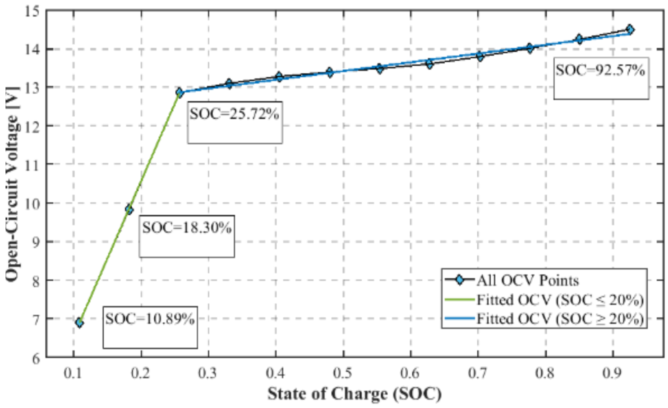

Fig. 3 – Battery open-circuit voltage characterization.

6.1. MEMORY LENGTH ANALYSIS

As previously discussed, the optimal memory length M_{opt} for the fractional derivative was determined based on both the AIC (24) and BIC (25) criteria across candidate memory lengths $L = 1\ldots20$.

As illustrated in Figure 4, both criteria demonstrate clear minimization patterns, with $M_{opt}^{AIC} = 5$and $M_{opt}^{BIC} = 4$.

The improvement from $M = 4$ to $M = 5$ was statistically insignificant:

$$\frac{\mathrm{RMSE}(M=5)}{\mathrm{RMSE}(M=4)} = 0.968 \geq 0.95. \tag{41}$$

Consequently, for this case, the selection $M_{opt}= 4$ is justified, balancing model fidelity against computational complexity. The identified FO-ECM parameters were used to simulate the battery's voltage response under the experimental discharge profiles. As depicted in Fig. 5, the model achieves acceptable average voltage tracking accuracy, with minor discrepancies observed at low SOC levels.

The observed discrepancies at low battery voltage are anticipated to be mitigated during online state estimation, as the EKF's recursive parameter adjustment capability continuously adapts the model to actual operating conditions. This adaptive compensation mechanism is demonstrated in the following subsection.

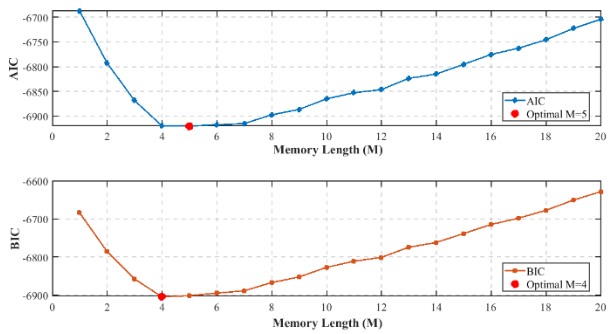

Fig. 4 – Optimal memory length selection using AIC and BIC criterions

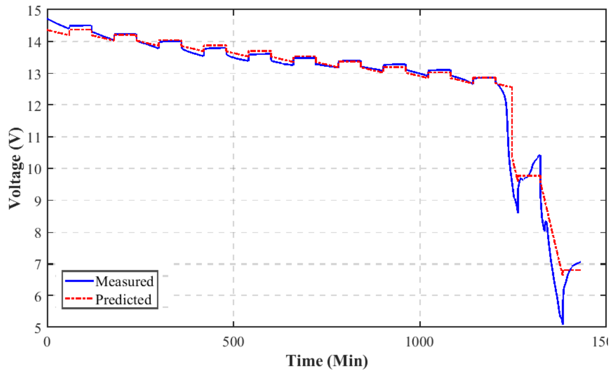

Fig. 5 – Model validation: measured versus simulated battery pack terminal voltage.

6.2. ONLINE BATTERY STATE ESTIMATION VIA EXTENDED KALMAN FILTER

The EKF initialized with offline-identified parameters, estimates battery state in real time.

Figure 6 shows results for successive discharge/rest cycles, demonstrating improved performance over static models.

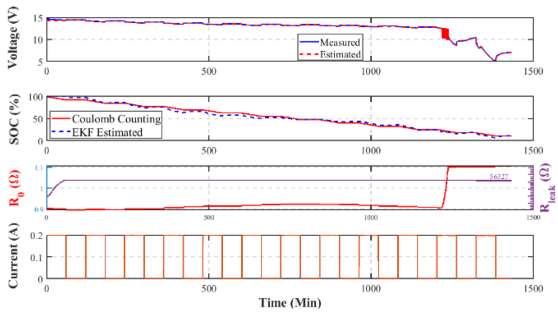

Fig. 6 – EKF estimation during discharge/rest cycles (voltage, SOC, and model resistances).

The EKF achieves SOC estimation with average RMSE of 3.5% (vs. Coulomb counting). Parameter tracking shows R_0 converging rapidly to a stable low value, while R_{leak} maintains its characteristic high value. This enables effective State-of-Health tracking without separate estimation routines [23].

6.3. BENCHMARK VALIDATION WITH DST AND FUDS PROFILES

Validation using CALCE benchmark data [24] on 2 Ah INR18650 cells considered two dynamic profiles: DST (dynamic stress test) and FUDS (federal urban driving schedule). Each test includes charging, relaxation, and discharge phases. To further assess the estimator's practical resilience, zero-mean Gaussian noise with a standard deviation of 1% was added to the measured current and voltage signals to simulate sensor imperfections and test the filter's inherent noise rejection.

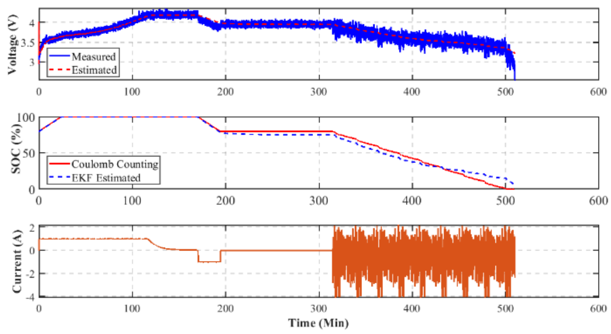

Fig. 7 – Cell voltage and SOC estimation during a DST test (temperature: 25°C).

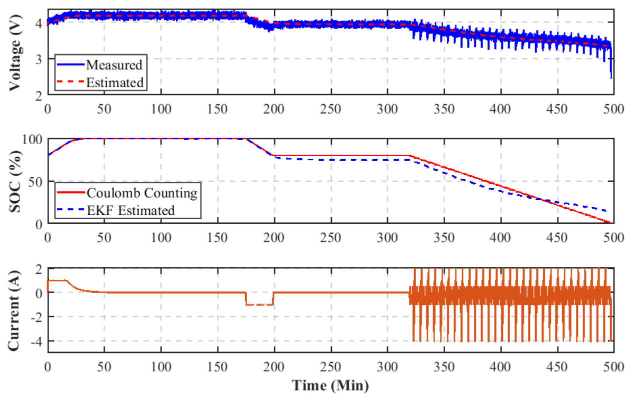

Fig. 8 – Cell voltage and SOC estimation during a FUDS test (temperature: 45°C).

The state estimation results for these demanding scenarios are shown in Figure 7 (DST profile at ambient temperature: 25°C) and Figure 8 (FUDS profile, at a temperature of 45°C).

Despite the compounded challenges posed by aggressive load dynamics, sensor noise, and temperature variations, the estimator maintained robust performance. It successfully tracked the terminal voltage and delivered an accurate, real-time estimate of the State of Charge.

The SOC estimation is achieved with an average RMSE of about 3.5% across all test conditions. These results confirm the efficiency and robustness of the proposed algorithm against environmental fluctuations and noisy measurement conditions.

7. CONCLUSIONS

This paper presents a unified framework for adaptive, high-fidelity state estimation in lithium-ion batteries, integrating a fractional-order equivalent circuit model with a joint state-parameter Extended Kalman Filter.

This system simultaneously estimates SOC and tracks degradation-sensitive parameters, addressing the limitations of conventional BMS algorithms—integer-order oversimplification and performance drift from fixed parameters.

The Grünwald-Letnikov-based FO-ECM captures distributed battery dynamics with parsimonious structure, while the joint EKF enables real-time self-correction and operational compensation.

The paper principal Contributions are:

- A robust sequential methodology identifies all model parameters from standard discharge/rest data, including criteria-based selection of optimal memory length balancing fidelity and computational load.

- The FO-ECM is embedded within an EKF with augmented state vector (SOC, R_0, R_{leak}), enabling inherent online adaptation and direct State-of-Health tracking without separate routines.

- Performance was validated on a 2.5 Ah battery pack and standardized DST/FUDS profiles at 25°C and 45°C with added 1% sensor noise—confirmed consistent robustness, with average SOC estimation RMSE consistently below 3.5% across all test scenarios.

Future work includes temperature as an additional estimated state, adaptive noise covariance tuning, embedded hardware implementation, and long-term aging studies for continuous State-of-Health tracking.

Received on 22 March 2026

REFERENCES

1. G. Feng et al., "A systematic review of electrochemical model-based lithium-ion battery state estimation in battery management systems," J. Energy Storage, **101**, pp. 113850 (2023).
2. N. Jan et al., "Investigation of the suitability of the DTV method for the online SoH estimation of NMC lithium-ion cells in battery management systems," Batteries, **11**, *1*, pp. 25 (2025).
3. J. Hosein et al., "Electrochemical modeling in lithium batteries: Pathways to next-generation power sources", J. Power Sources, **564**, pp. 237833 (2025).
4. S.A. Lupu, D. Floricău, "The influence of temperature at charging and discharging the Li-ion battery," Rev. Roum. Sci. Techn. – Électrotechn. et Énerg., **70**, *1*, pp. 91–96 (2025).
5. J. Meng et al., "Overview of lithium-ion battery modeling methods for state-of-charge estimation in electric vehicles," Appl. Sci., **8**, *5*, pp. 609–619 (2018).
6. M.Q. Lili et al., "Co-estimation of state of charge and state of health for lithium-ion batteries based on fractional-order model with multi-innovations unscented Kalman filter method," J. Energy Storage, **52**, pp. 104904 (2022).
7. A. Oustaloup et al., "Frequency-band complex noninteger differentiator: Characterization and synthesis," IEEE Trans. Circuits Syst. I, **47**, *1*, pp. 25–39 (2000).
8. A. Allagui et al., "Reevaluation of performance of electric double-layer capacitors from constant-current charge/discharge and cyclic voltammetry," Sci. Rep., **6**, pp. 38568 (2018).
9. Z. He et al., "State-of-charge estimation of lithium ion batteries based on adaptive iterative extended Kalman filter," J. Energy Storage, **39**, pp. 102593 (2021).
10. S.M.M. Alavi et al., "Time-domain fitting of battery electrochemical impedance models," J. Power Sources, **288**, pp. 345–352 (2015).
11. C. Zhang et al., "Online estimation of battery equivalent circuit model parameters and state of charge using decoupled least squares technique," Energy, **142**, pp. 678–688 (2018).
12. G. Jasmine, T. Venkatraman, B.M.S Natarajan, R. Manidevesh, "Electric vehicle onboard charging via Harris Hawks optimization-based on fractional-order sliding mode controller," Rev. Roum. Sci. Techn. – Électrotechn. et Énerg., **68**, *1*, pp. 30–35 (2023).
13. G. Jasmine, T. Venkatraman, B.M.S Natarajan, N. Muthukumaran, M. Veluchamy, "Red Fox-based fractional order fuzzy PID controller for smart LED driver circuit," Rev. Roum. Sci. Techn. – Électrotechn. et Énerg., **68**, *4*, pp. 394–399 (2023).
14. D. Chouaibi, W. Chagra, "A new hybrid optimization method used in predictive control of a nonlinear fractional model based on fractional Hammerstein structure," Rev. Roum. Sci. Techn. – Électrotechn. et Énerg., **69**, *4*, pp. 437–442 (2024).
15. A. Djeddi, T. Amieur, F. Hannahi, S. Metatla, A. Aouiche, "Synthesis of fractional order fuzzy observer for a fractional order Takagi-Sugeno model with unmeasurable premise variables," Rev. Roum. Sci. Techn. – Électrotechn. et Énerg., **69**, *1*, pp. 45–50 (2024).
16. R. Ranjith Kumar et al., "Advances in batteries, battery modeling, battery management system, battery thermal management, SOC, SOH, and charge/discharge characteristics in EV applications," IEEE Access, **11**, pp. 105761–105809 (2023).
17. S. Guermah et al., "Discrete-time fractional-order systems: Modeling and stability issues," in *Advances in Discrete Time Systems*, IntechOpen, pp. 183–212 (2012).
18. H. Akaike, "A new look at the statistical model identification," IEEE Trans. Autom. Control, **19**, *6*, pp. 716–723 (1974).
19. G. Schwarz, "Estimating the dimension of a model," Ann. Statist., **6**, *2*, pp. 461–464 (1978).
20. Y. Liang et al., "An error covariance correction-adaptive extended Kalman filter based on piecewise forgetting factor recursive least squares method for the state-of-charge estimation of lithium-ion batteries," J. Energy Storage, **68**, pp. 107629 (2023).
21. D. Sierociuk et al., "Fractional Kalman filter algorithm for the states, parameters and order of fractional system estimation," Int. J. Appl. Math. Comput. Sci., **16**, *1*, pp. 129–140 (2006).
22. E.H. Bensikaddour, A. Boutte, "Proposal of battery management strategy for small geostationary satellite power system development," Rev. Roum. Sci. Techn. – Électrotechn. et Énerg., **67**, *2*, pp. 151–156 (2022).
23. S.J. Moura et al., "Adaptive PDE observer for battery SOC/SOH estimation via an electrochemical model," J. Dyn. Syst. Meas. Control, **136**, *1*, pp. 011015 (2014).
24. ***Center for Advanced Life Cycle Engineering (CALCE), "Battery data" [Data set], University of Maryland (2025).